NASA TECHNICAL NOTE

NASA TN D-8318

NASA TN D-8318

ISOTHERMAL ELASTOHYDRODYNAMIC LUBRICATION OF POINT CONTACTS

IV - Starvation Results

Bernard J. Hamrock and Duncan Dowson

Lewis Research Center
Cleveland, Ohio 44135

NATIONAL AERONAUTICS AND SPACE ADMINISTRATION • WASHINGTON, D. C. • OCTOBER 1976

1. Report No. NASA TN D-8318	2. Government Accession No.	3. Recipient's Catalog No.

4. Title and Subtitle
ISOTHERMAL ELASTOHYDRODYNAMIC LUBRICATION OF POINT CONTACTS
IV - STARVATION RESULTS

5. Report Date
October 1976

6. Performing Organization Code

7. Author(s)
Bernard J. Hamrock of the Lewis Research Center; and
Duncan Dowson of the University of Leeds

8. Performing Organization Report No.
E-8733

10. Work Unit No.
505-04

9. Performing Organization Name and Address
Lewis Research Center
National Aeronautics and Space Administration
Cleveland, Ohio 44135

11. Contract or Grant No.

13. Type of Report and Period Covered
Technical Note

12. Sponsoring Agency Name and Address
National Aeronautics and Space Administration
Washington, D.C. 20546

14. Sponsoring Agency Code

15. Supplementary Notes

16. Abstract
The theory and numerical procedure developed by the authors in an earlier publication were used to investigate the influence of lubricant starvation on minimum film thickness. This study of lubricant starvation was performed simply by moving the inlet boundary closer to the contact center. From the results it was found that, for the range of conditions considered, dimensionless inlet distance at the boundary between the fully flooded and starved conditions m^* can be expressed simply as $m^* = 1 + 3.06\left[(R_x/b)^2 H_{c,F}\right]^{0.58}$, where R_x is the effective radius of curvature, b is the semiminor axis of the contact ellipse, and $H_{c,F}$ is the central film thickness for fully flooded conditions, or $m^* = 1 + 3.34\left[(R_x/b)^2 H_{min,F}\right]^{0.56}$, where $H_{min,F}$ is the minimum film thickness for fully flooded conditions. That is, for a dimensionless inlet distance m less than m^*, starvation occurs; and for $m \geq m^*$, a fully flooded condition exists. Furthermore, it has been possible to express the central and minimum film thicknesses for a starved condition as $H_{c,S} = H_{c,F}\left[(m - 1)/(m^* - 1)\right]^{0.29}$ and $H_{min,S} = H_{min,F}\left[(m - 1)/(m^* - 1)\right]^{0.25}$. Contour plots of the pressure and the film thickness in and around the contact are shown for the fully flooded and starved lubricating conditions. From these contour plots it was observed that the pressure spike becomes suppressed and the film thickness decreases substantially as starvation increases.

17. Key Words (Suggested by Author(s))
Elastohydrodynamics
Lubrication
Bearings
Gears

18. Distribution Statement
Unclassified - unlimited
STAR Category 37

19. Security Classif. (of this report)	20. Security Classif. (of this page)	21. No. of Pages	22. Price*
Unclassified	Unclassified	32	$4.00

* For sale by the National Technical Information Service, Springfield, Virginia 22161

ISOTHERMAL ELASTOHYDRODYNAMIC LUBRICATION OF POINT CONTACTS

IV - STARVATION RESULTS*

by Bernard J. Hamrock and Duncan Dowson†

Lewis Research Center

SUMMARY

The theory and numerical procedure developed by the authors in an earlier publication were used to investigate the influence of lubricant starvation on minimum film thickness. This study of lubricant starvation was performed simply by moving the inlet boundary closer to the contact center. From the results it was found that, for the range of conditions considered, dimensionless inlet distance at the boundary between the fully flooded and starved conditions m^* can be expressed simply as $m^* = 1 + 3.06 \left[(R_x/b)^2 H_{c,F}\right]^{0.58}$, where R_x is the effective radius of curvature, b is the semiminor axis of the contact ellipse, and $H_{c,F}$ is the central film thickness for fully flooded conditions, or $m^* = 1 + 3.34 \left[(R_x/b)^2 H_{min,F}\right]^{0.56}$, where $H_{min,F}$ is the minimum film thickness for fully flooded conditions. That is, for a dimensionless inlet distance m less than m^*, starvation occurs; and for $m \geq m^*$, a fully flooded condition exists. Furthermore, it has been possible to express the central and minimum film thicknesses for a starved condition as $H_{c,S} = H_{c,F} \left[(m - 1)/(m^* - 1)\right]^{0.29}$ and $H_{min,S} = H_{min,F} \left[(m - 1)/(m^* - 1)\right]^{0.25}$. Contour plots of the pressure and the film thickness in and around the contact are shown for the fully flooded and starved lubricating conditions. From these contour plots it was observed that the pressure spike becomes suppressed and the film thickness decreases substantially as starvation increases.

*Presented at Joint Lubrication Conference cosponsored by the American Society of Mechanical Engineers and the American Society of Lubrication Engineers, Boston, Massachusetts, October 5-7, 1976.

†Professor of Mechanical Engineering, University of Leeds, Leeds, England.

INTRODUCTION

It was not until the late 1960's and early 1970's that the influence of lubricant starvation upon elastohydrodynamic behavior received serious consideration. Prior to this time it was assumed that the inlets were fully flooded. This assumption seemed to be entirely reasonable in view of the minute quantities of lubricant required to provide an adequate film. However, in due course it was recognized that some machine elements suffered from lubricant starvation.

How partial filling of the inlet to an elastohydrodynamic conjunction influences pressure and film thickness can readily be explored theoretically by adopting different starting points for the inlet pressure boundary. Orcutt and Cheng (ref. 1) appear to have been the first to proceed in this way for a specific case corresponding to a particular experimental situation. Their results showed that lubricant starvation lessened the film thickness. Wolveridge, et al. (ref. 2) used a Grubin approach (ref. 3) in an analysis of starved elastohydrodynamic lubricated line contacts. Wedeven, et al. (ref. 4) analyzed a starved condition in a ball-on-plate geometry configuration, and Castle and Dowson (ref. 5) presented a numerical solution for the starved line-contact elastohydrodynamic situation. In both references 2 and 4 the analysis yielded values of the proportional reduction in centerline film thickness from the fully flooded condition in terms of a dimensionless inlet boundary parameter.

Only in recent years have complete solutions of the isothermal elastohydrodynamic lubrication (EHL) of point contacts been presented. The analysis requires the simultaneous solution of the elasticity and Reynolds equations. The authors' approach to the theoretical solution is presented in two previous publications (refs. 6 and 7). The first of these publications (ref. 6) presents an elasticity model in which the conjunction is divided into equal rectangular areas with a uniform pressure applied over each area. The second (ref. 7) gives a complete approach to solving the elastohydrodynamic lubrication problem for point contacts.

The most important practical aspect of the EHL point-contact theory (ref. 7) is the determination of the minimum film thickness within the contact. That is, the maintenance of a sufficient fluid film is extremely important to the operation of the machine elements in which these thin, continuous, fluid films occur. In a recent report by the authors (ref. 8) the fully flooded results obtained from the theory given in references 6 and 7 are presented. In the results the influence of the ellipticity and dimensionless speed, load, and material parameters on minimum film thickness was investigated. Thirty-four different cases were used in obtaining the fully flooded minimum-film-thickness formula.

The present report uses the basic theory developed in references 6 and 7 in studying the effect of lubricant starvation on pressure and film thickness within the conjunction. The objective of this work is to provide a simple expression for the dimensionless inlet

boundary distance. This inlet boundary distance defines whether a fully flooded or a starved condition exists in the contact. An additional objective is to develop simple expressions for the minimum and central film thicknesses under the starvation condition. Fifteen cases, in addition to three presented in reference 8, were used in obtaining the starvation results. To more fully understand what occurs in going from a fully flooded condition to a lubricant starvation condition, contour plots of pressure and film thickness in and around the contact are shown. The theoretical findings are compared with previously reported results.

SYMBOLS

A	constant defined in eq. (2)
a	semimajor axis of contact ellipse
B	constant defined in eq. (2)
b	semiminor axis of contact ellipse
E	modulus of elasticity
E'	$\dfrac{2}{\dfrac{1-\nu_A^2}{E_A}+\dfrac{1-\nu_B^2}{E_B}}$
F	normal applied load
G	dimensionless material parameter, $E'/p_{iv,as}$
$H_{c,F}$	dimensionless film thickness at center of contact for a fully flooded conjunction, h_c/R_x
H_{min}	dimensionless minimum film thickness, h_{min}/R_x
$H_{min,F}$	dimensionless minimum film thickness for a fully flooded conjunction, $h_{min,F}/R_x$
$\tilde{H}_{min,S}$	dimensionless minimum film thickness for a starved conjunction as obtained from least-square fit of data, $\tilde{h}_{min,S}/R_x$
h	film thickness
k	ellipticity parameter, a/b
m	dimensionless inlet distance
m^*	dimensionless inlet distance at boundary between fully flooded and starved conditions

m_W	dimensionless inlet distance boundary as obtained from Wedeven, et al. (ref. 4)
P	dimensionless pressure, p/E'
p	pressure
$p_{iv,as}$	asymptotic isoviscous pressure
R	effective radius of curvature
r	radius of curvature
U	dimensionless speed parameter, $u\eta_0/E'R_x$
u	surface velocity in x-direction
W	dimensionless load parameter, $F/E'R_x^2$
$x,X,\overline{X}$ $y,Y,\overline{Y}$	coordinate systems defined in report
α	pressure-viscosity coefficient
η_o	atmospheric viscosity
ν	Poisson's ratio

Subscripts:

A	solid A
B	solid B
x,y	coordinate system defined in report

BOUNDARY BETWEEN FULLY FLOODED AND STARVED CONDITIONS

Figure 1 shows the computing area in and around the Hertzian contact. In this figure the coordinate X is made dimensionless with respect to the semiminor axis b of the contact ellipse, and the coordinate Y is made dimensionless with respect to the semimajor axis a of the contact ellipse. The ellipticity parameter k is defined as the semimajor axis divided by the semiminor axis of the contact ellipse (k = a/b). Because of the way the coordinates X and Y are made dimensionless, the Hertzian contact ellipse becomes a Hertzian circle regardless of the ellipticity parameter. This Hertzian contact circle is shown in figure 1 with a radius of unity. The edges of the computing area, where the pressure is assumed to be ambient, are also denoted. In this figure the dimensionless inlet distance m, which is equal to the dimensionless distance from the center of contact to the inlet edge of the computing area, is shown.

Lubricant starvation can be studied simply by reducing the dimensionless inlet distance. A fully flooded condition is said to exist when the dimensionless inlet distance ceases to influence in any significant way the minimum film thickness. When starting from a fully flooded condition and decreasing m, the value at which the minimum film thickness first starts to change is called the fully flooded - starved boundary and is denoted by m^*. Therefore, lubricant starvation was studied by using the basic elastohydrodynamic lubrication point-contact theory developed in reference 7 and observing the effect of reducing the dimensionless inlet distance.

Table I shows how changing the dimensionless inlet distance affects the dimensionless minimum film thickness for three groups of dimensionless load and speed parameters. For all the results presented in this report the material parameter G is fixed at 4522 and the ellipticity parameter is fixed at 6. In this table it is seen that as the dimensionless inlet distance m decreases the dimensionless minimum film thickness H_{min} decreases.

Table II shows how the three groups of dimensionless speed and load parameters affect the location of the dimensionless inlet boundary m^*. Also given in this table are the corresponding values of the dimensionless central and minimum film thicknesses for the fully flooded condition as obtained by interpolation of the numerical values. The dimensionless inlet boundary distance m^* shown in table II was obtained by using the data from table I when the following equation was satisfied:

$$\frac{H_{min,F} - \left(H_{min}\right)_{m=m^*}}{H_{min,F}} = 0.03 \tag{1}$$

The value of 0.03 is used in equation (1) since it was ascertained that the data in table I could only be obtained to an accuracy of 3 percent.

The general form of the equation that describes how the dimensionless inlet distance at the fully flooded - starved boundary varies is given as

$$m^* - 1 = A\left[\left(\frac{R_x}{b}\right)^2 H_{c,F}\right]^B \tag{2}$$

The right side of equation (2) is similar to the forms of the equation given by Wolveridge, et al. (ref. 2) and Wedeven, et al. (ref. 4). By using the data obtained from table I, the following equation can be written:

$$m^* = 1 + 3.06\left[\left(\frac{R_x}{b}\right)^2 H_{c,F}\right]^{0.58} \tag{3}$$

A fully flooded condition exists when $m \geq m^*$, and a starved condition exists when $m < m^*$.

If in equation (2) the dimensionless minimum film thickness is used instead of the central film thickness, the following equation is obtained:

$$m^* = 1 + 3.34\left[\left(\frac{R_x}{b}\right)^2 H_{min,F}\right]^{0.56} \tag{4}$$

From Wedeven, et al. (ref. 4), using the symbols of this report, the dimensionless inlet distance at the fully flooded - starved boundary can be written as

$$m_W = 1 + 3.52\left[\left(\frac{R_x}{b}\right)^2 H_{c,F}\right]^{2/3} \tag{5}$$

Comparing equation (3) with equation (5) indicates close agreement with reference 4. Wedeven, however, predicts a slightly higher value of the fully flooded - starved boundary than is predicted from the present results.

FILM-THICKNESS FORMULAS

Having clearly established the limiting location of the inlet boundary for the fully flooded condition (eqs. (3) and (4)), an equation defining the dimensionless central film thickness for lubricant starvation conditions will be developed. The relation between the dimensionless central film thickness in the starved and fully flooded conditions can be expressed in general form as

$$\frac{H_{c,S}}{H_{c,F}} = C\left(\frac{m - 1}{m^* - 1}\right)^D \tag{6}$$

Table III shows how the ratio of the dimensionless inlet distance parameter to the fully flooded - starved boundary $(m - 1)/(m^* - 1)$ affects the ratio of central film thick-

ness in the starved and fully flooded conditions $H_{c,S}/H_{c,F}$. A least-square power curve fit to the 16 pairs of data points

$$\left(\frac{H_{c,S}}{H_{c,F}}\right)_i, \left(\frac{m - 1}{m^* - 1}\right)_i \qquad \text{where } i = 1,2, \ldots, 16$$

was used in obtaining the dimensionless central film thickness for a starved condition

$$H_{c,S} = H_{c,F}\left(\frac{m - 1}{m^* - 1}\right)^{0.29} \tag{7}$$

By using a similar approach while making use of the data in table III, the dimensionless minimum film thickness for a starved condition can be written as

$$H_{min,S} = H_{min,F}\left(\frac{m - 1}{m^* - 1}\right)^{0.25} \tag{8}$$

Therefore, whenever $m < m^*$, where m^* is defined by either equation (3) or (4), a lubricant starvation condition exists. When this is true, the dimensionless central film thickness is expressed by equation (7) and the dimensionless minimum film thickness is expressed by equation (8). If $m \geq m^*$, where m^* is defined by either equation (3) or (4), a fully flooded condition exists. The dimensionless central and minimum film thicknesses for a fully flooded condition ($H_{c,F}$ and $H_{min,F}$) were developed in reference 8 and can be written as

$$H_{c,F} = 2.69\, U^{0.67} G^{0.53} W^{-0.067}(1 - 0.61\, e^{-0.73k}) \tag{9}$$

$$H_{min,F} = 3.63\, U^{0.68} G^{0.49} W^{-0.073}(1 - e^{-0.68k}) \tag{10}$$

where the dimensionless speed parameter

$$U = \frac{\eta_o u}{E' R_x} \tag{11}$$

the dimensionless load parameter

$$W = \frac{F}{E'R_x^2} \tag{12}$$

the dimensionless material parameter

$$G = \frac{E'}{p_{iv,as}} \tag{13}$$

the dimensionless ellipticity parameter

$$k = \frac{a}{b} \tag{14}$$

Equations (13) and (14) can be expressed in a more usable form as

$$G = E'\alpha \tag{15}$$

$$k = 1.03\left(\frac{R_y}{R_x}\right)^{0.64} \tag{16}$$

In equation (16) the ellipticity parameter is expressed strictly in terms of the radii of curvature and thereby eliminates the common practice of evaluating the elliptical integrals of the first and second kinds.

The ratio of the dimensionless inlet distance to the fully flooded - starved boundary as obtained from Wedeven, et al. (ref. 4), expressed as $(m - 1)/(m_W - 1)$, is also given in table III. By comparing these results with the results obtained from the present work, $(m - 1)/(m^* - 1)$, it can be seen that for group 1 the agreement is excellent. However, the agreement in groups 2 and 3 is not as good. A possible explanation for this difference can be that in the Wedeven, et al. (ref. 4) analysis, an approximate expression for the Hertzian deformation is used. They indicate that their equation (eq. (5)) is only valid for small m^* or more specifically $m^* < 3$. In group 2, $m^* = 3.71$; and in group 3, $m^* = 5.57$. Since no such assumption is required in deriving equations (3) and (4), they would seem to be more appealing.

Figure 2 shows the influence of inlet boundary parameter upon central film thickness for the Wedeven, et al. (ref. 4) results and for those obtained from the present work. From this figure it is observed that the Wedeven, et al. (ref. 4) results give slightly higher values of the central-film-thickness ratio of starved to fully flooded conditions than those obtained from the present results.

CONTOUR PLOTS OF RESULTS

To explain more fully what happens in going from a fully flooded to a lubricant starvation condition, figures 3 to 8 are presented. In figures 3(a), (b), and (c) contour plots of dimensionless pressure ($P = p/E'$) are given for group 1 of table II and for dimensionless inlet distances of 4, 2, and 1.25, respectively. In these figures and the remainder of the contour plots to be presented the symbol + indicates the center of the Hertzian contact. It should be remembered that because of the way the coordinates are made dimensionless, the actual contact ellipse becomes a Hertzian circle regardless of the ellipticity parameter. The Hertzian contact circle is shown in each figure by asterisks. At the top of each figure the contour label and its corresponding value are given. The inlet region is to the left and the exit region is to the right.

In figure 3 the contour values were kept constant. In figures 3(a) and (b) the pressure spikes are shown with the B and C contour labels, respectively; and in figure 3(c) no pressure spike occurs. This implies that as the dimensionless inlet distance m decreases (or as starvation occurs) the pressure spike is suppressed. In figure 3(a), with $m = 4$, a fully flooded condition exists. In figure 3(b), with $m = 2$, a starved condition exists. And in figure 3(c), with $m = 1.25$, the starvation is even more severe. That is, once starvation occurs the severity of the situation increases as m is decreased. Note in figure 3(c), the most severe starvation case, that the contour labeled H does not extend as far to the left as it did for the fully flooded pressure results shown in figure 3(a).

In figures 4(a), (b), and (c) contour plots of dimensionless film thickness ($H = h/R_x$) are given for group 1 of table II and dimensionless inlet distances m of 4, 2, and 1.25, respectively. These film-thickness results correspond to the pressure results shown in figure 3. The central portion of the film-thickness contours has become more parallel as starvation has increased (figs. 4(a) to (c)), with the minimum film area decreasing. Note also that the film-thickness contour values for the starved condition (fig. 4(c)) are much lower than those for the fully flooded condition (fig. 4(a)).

In figures 5(a), (b), and (c) contour plots of dimensionless pressure ($P = p/E'$) are given for group 3 of table II and dimensionless inlet distances m of 6, 2.5, and 1.5, respectively. This set of results should be compared with those presented for the lower speed parameter U in figure 3. The contour values in figures 5(a), (b), and (c) are the same in each case. In figure 5(a) a fully flooded condition exists, while in figure 5(c) a severely starved condition exists. The following observations can be made about figure 5:

(1) The distance from the center of the contact to the upstream location of the largest contour (labeled H) decreases as the severity of lubricant starvation increases.

(2) Contours A, B, and C are absent in the severely starved condition (fig. 5(c)).

Contour plots of the dimensionless film thickness ($H = h/R_x$) are shown for group 3 of table II and for dimensionless inlet distances m of 6, 2.5, and 1.5, respectively, in

figures 6(a), (b), and (c). These film-thickness results correspond to the pressure results shown in figure 5. In figure 6(a) (the fully flooded condition) the minimum film area occurs to the sides of the conjunction in two areas that are midway between the center of the contact and the Hertzian circle. In figure 6(c) (the severely starved condition) the central portion has roughly parallel contours in the direction of motion with one minimum area directly behind the axial center of the contact and near the Hertzian circle. Ranger, et al. (ref. 9) also found a similar contour plot in their 1975 publication. Note the similarity between the film-thickness contours of figure 4(c) (group 1 of table II) and that of figure 6(c) (group 3 of table II). From the labels of the contours in figure 6 we see that the film thickness for the starved condition is much lower than the film thickness in the fully flooded condition.

The dimensionless pressure ($P = p/E'$) on the $\overline{X}$-axis is shown for three values of dimensionless inlet distance m and for groups 1 and 3 of table II, respectively, in figures 7(a) and (b). The value of Y is held constant near the axis of symmetry of the conjunction. In these figures as a conjunction becomes starved (as m is decreased) the pressure spike diminishes.

Figures 8(a) and (b) show the dimensionless film thickness ($H = h/R_x$) on the $\overline{X}$-axis for three values of the dimensionless inlet distance m and for groups 1 and 3 of table II, respectively. The value of Y is held fixed close to the axis of symmetry of the contact. In these figures, particularly figure 8(b), the central region becomes flatter as starvation occurs. Also, in going from a fully flooded condition to a starved condition the film thickness decreases substantially.

CONCLUDING REMARKS

By using the theory and numerical procedure outlined and developed by the authors in earlier publications, the influence of lubricant starvation upon minimum film thickness in starved elliptical elastohydrodynamic conjunctions has been investigated. This study of lubricant starvation was performed simply by moving the inlet boundary closer to the center of the conjunction. From the results it was found that the location of the dimensionless inlet boundary m^* between the fully flooded and starved conditions could be expressed simply as

$$m^* = 1 + 3.06\left[\left(\frac{R_x}{b}\right)^2 H_{c,F}\right]^{0.58}$$

or

$$m^* = 1 + 3.34\left[\left(\frac{R_x}{b}\right)^2 H_{min,F}\right]^{0.56}$$

That is, for a dimensionless inlet distance m less than m*, starvation occurs; and for $m \geq m^*$, a fully flooded condition exists. Furthermore, it has been possible to express the central and minimum film thicknesses for a starved condition as

$$H_{c,S} = H_{c,F}\left(\frac{m - 1}{m^* - 1}\right)^{0.29}$$

$$H_{min,S} = H_{min,F}\left(\frac{m - 1}{m^* - 1}\right)^{0.25}$$

where

$H_{c,F}$	fully flooded dimensionless central film thickness
$H_{min,F}$	fully flooded dimensionless minimum film thickness
m	dimensionless inlet distance
m*	dimensionless inlet distance at the fully flooded - starved boundary

Contour plots of the pressure and the film thickness in and around the contact have been presented for both the fully flooded and starved lubrication conditions. It is evident from the contour plots that the pressure spike becomes suppressed and the film thickness decreases substantially as the severity of starvation increases.

The results presented in this report, when combined with the findings previously reported, enable the essential features of starved, elliptical elastohydrodynamic conjunctions to be ascertained.

Lewis Research Center,
National Aeronautics and Space Administration,
Cleveland, Ohio, July 28, 1976,
505-04.

REFERENCES

1. Orcutt, F. K.; and Cheng, H. S.: Lubrication of Rolling-Contact Instrument Bearings. Gryo-Spin Axis Hydrodynamic Bearing Symposium, Vol. 2, Mass. Inst. Technol. Instru. Lab., 1966.

2. Wolveridge, P. E.; Baglin, K. P.; and Archard, J. G.: The Starved Lubrication of Cylinders in Line Contact. Proc. Inst. Mech. Eng., vol. 185, 1971, pp. 1159-1169.

3. Grubin, A. N.; and Vinogradova, I.E., eds.: Investigation of the Contact of Machine Components. Book 30. CTS-235, Central Res. Inst. Technol. Mech. Eng. (Moscow), 1949; D.S.I.R. Translation No. 337.

4. Wedeven, L. D.; Evans, D.; and Cameron, A.: Optical Analysis of Ball Bearing Starvation. J. Lub. Tech. (Trans ASME, ser. F), vol. 93, no. 3, July 1971, pp. 349-363.

5. Castle, P.; and Dowson, D.: Theoretical Analysis of the Starved Elastohydrodynamic Lubrication Problem for Cylinders in Line Contact. Elastohydrodynamic Lubrication. Inst. Mech. Engrs., 1972, pp. 131-137.

6. Hamrock, Bernard J.; and Dowson, Duncan: Numerical Evaluation of the Surface Deformation of Elastic Solids Subjected to a Hertzian Contact Stress. NASA TN D-7774, 1974.

7. Hamrock, Bernard J.; and Dowson, Duncan: Isothermal Elastohydrodynamic Lubrication of Point Contacts. I - Theoretical Formulation. NASA TN D-8049, 1975; also J. Lub. Tech. (Trans. ASME, ser. F), vol. 98, Apr. 1976, pp. 223-229.

8. Hamrock, Bernard J.; and Dowson, Duncan: Isothermal Elastohydrodynamic Lubrication of Point Contacts. III - Fully Flooded Results. NASA TN D-8317, 1976.

9. Ranger, A. P.; Ettles, C. M. M.; and Cameron, A.: The Solution of the Point Contact Elasto-Hydrodynamic Problem. Proc. Roy. Soc. (London), vol. 346A, no. 1645, Oct. 1975, pp. 227-244.

TABLE I. - EFFECT OF STARVATION ON MINIMUM FILM THICKNESS FOR THREE GROUPS OF THE DIMENSIONLESS SPEED AND LOAD PARAMETERS

Dimensionless inlet distance, m	Group		
	1	2	3
	Dimensionless load parameter, W		
	0.3686×10^{-6}	0.7371×10^{-6}	0.7371×10^{-6}
	Dimensionless speed parameter, U		
	0.1683×10^{-11}	1.683×10^{-11}	5.050×10^{-11}
	Minimum film thickness, H_{min}		
6	----------	29.75×10^{-6}	61.32×10^{-6}
4	6.317×10^{-6}	29.27	57.50
3	6.261	27.84	51.70
2.5	----------	26.38	46.89
2	5.997	23.46	39.91
1.75	----------	21.02	34.61
1.5	5.236	----------	27.90
1.25	3.945	----------	----------

TABLE II. - EFFECT OF DIMENSIONLESS SPEED AND LOAD PARAMETERS ON DIMENSIONLESS INLET DISTANCE AT FULLY FLOODED - STARVED BOUNDARY

Group	Dimensionless speed parameter, U	Dimensionless load parameter, W	Dimensionless radius parameter, R_x/b	Fully flooded central film thickness, $H_{c,F}$	Fully flooded minimum film thickness, $H_{min,F}$	Dimensionless inlet distance at fully flooded - starved boundary, m*
1	0.1683×10^{-11}	0.3686×10^{-6}	205.9	7.480×10^{-6}	6.221×10^{-6}	2.62
2	1.683	.7371	163.5	33.55	29.20	3.71
3	5.050	.7371	163.5	70.67	60.92	5.57

TABLE III. - EFFECT OF DIMENSIONLESS INLET DISTANCE ON DIMENSIONLESS CENTRAL AND MINIMUM FILM THICKNESS RATIOS

Group	Dimensionless inlet distance, m	Ratio of central film thicknesses for starved and flooded conditions, $H_{c,S}/H_{c,F}$	Ratio of minimum film thicknesses for starved and flooded conditions, $H_{min,S}/H_{min,F}$	Inlet boundary parameter, $(m - 1)/(m^* - 1)$	Inlet boundary parameter of Wedeven, et al. (1971), $(m - 1)/(m_W - 1)$
1	2.62	1	1	1	0.9895
	2	.9430	.9640	.6173	.6108
	1.5	.7697	.8417	.3086	.3054
	1.25	.5689	.6341	.1543	.1527
2	3.71	1	1	1	0.8281
	3	.9574	.9534	.7380	.6111
	2.5	.8870	.9034	.5535	.4584
	2	.7705	.8034	.3690	.3056
	1.75	.7151	.7199	.2768	.2292
3	5.57	1	1	1	0.8498
	4	.9348	.9439	.6565	.5579
	3	.8330	.8487	.4376	.3719
	2.5	.7440	.7697	.3282	.2789
	2	.6223	.6551	.2188	.1860
	1.75	.5309	.5681	.1641	.1395
	1.5	.4155	.4580	.1094	.0930

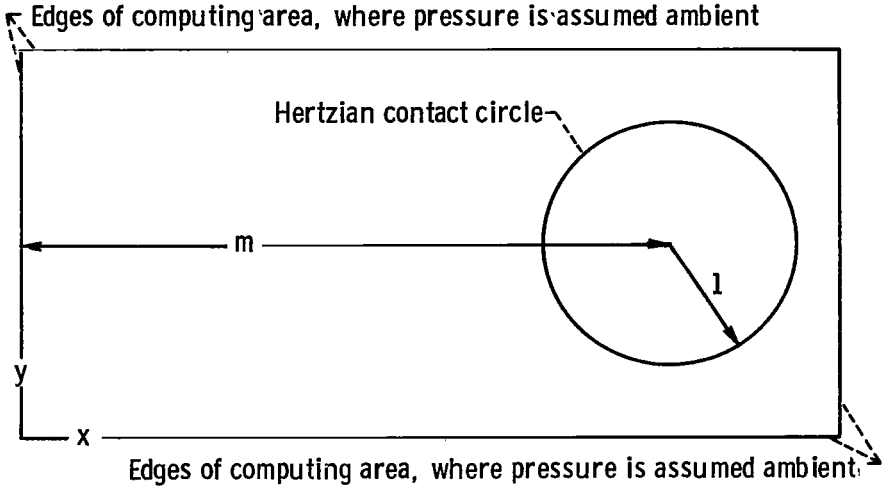

Figure 1. - Computing area in and around the Hertzian contact circle.

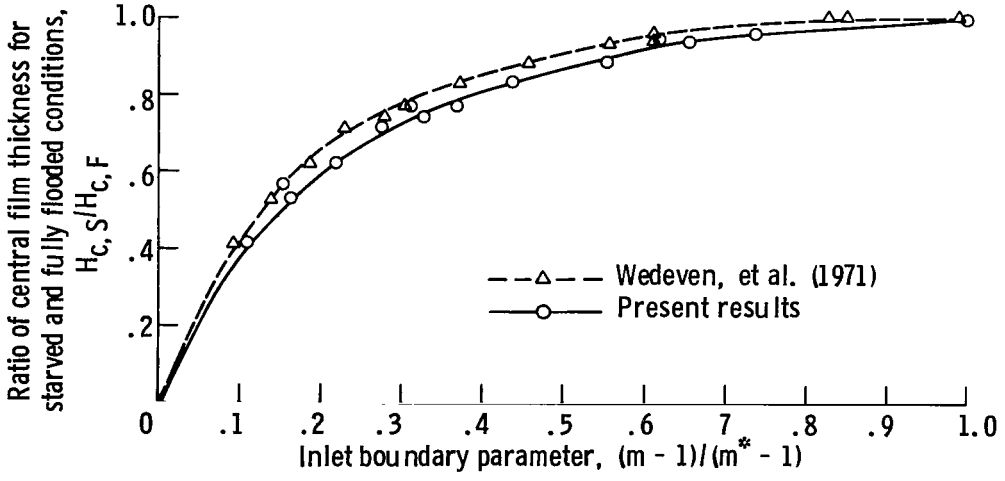

Figure 2. - Influence of inlet boundary parameter upon central-film-thickness ratio.

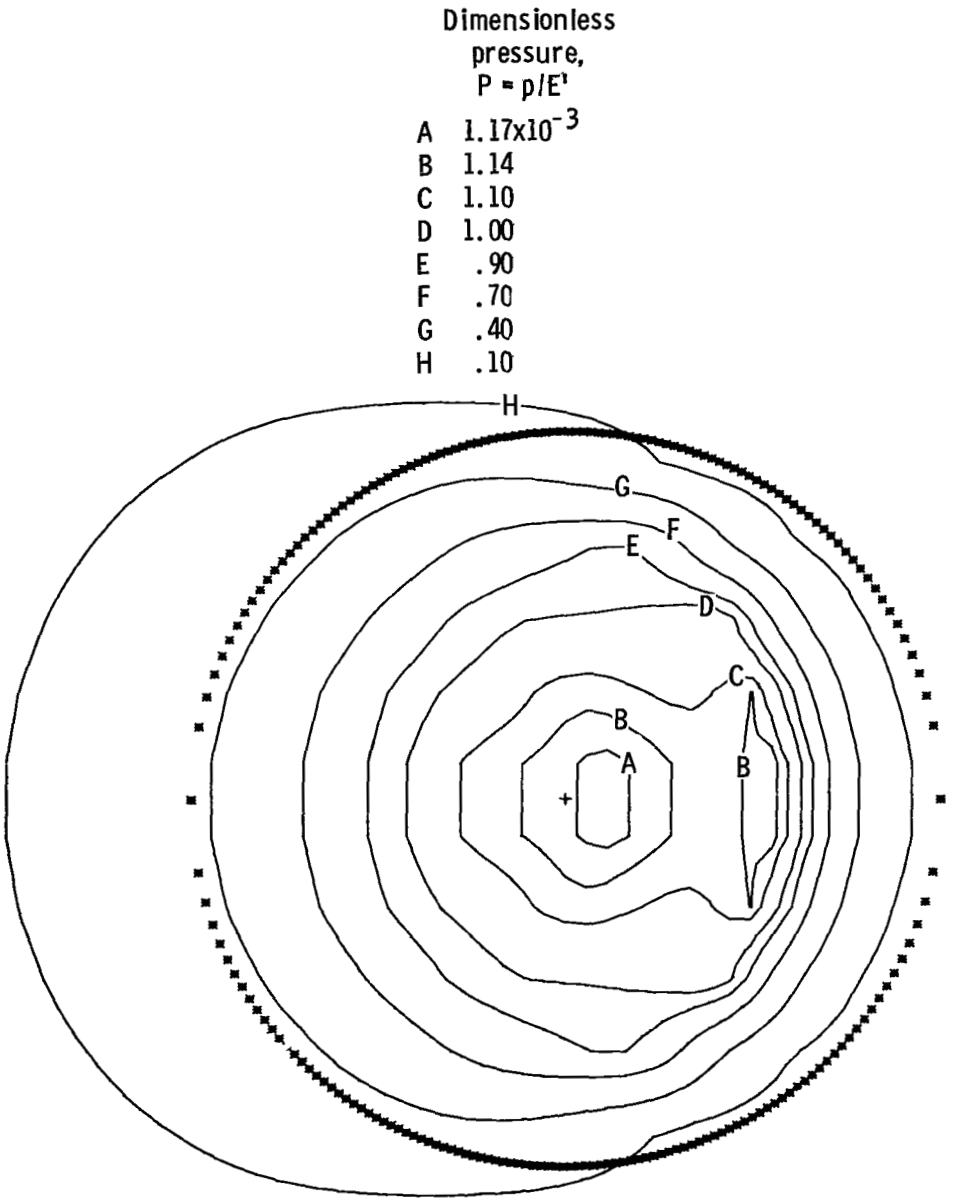

(a) m = 4.

Figure 3. - Contour plots of dimensionless pressure for dimensionless inlet distances m of 4, 2, and 1.25 and for group 1 of table II.

Dimensionless pressure, $P = p/E'$

A	1.17×10^{-3}
B	1.14
C	1.10
D	1.00
E	.90
F	.70
G	.40
H	.10

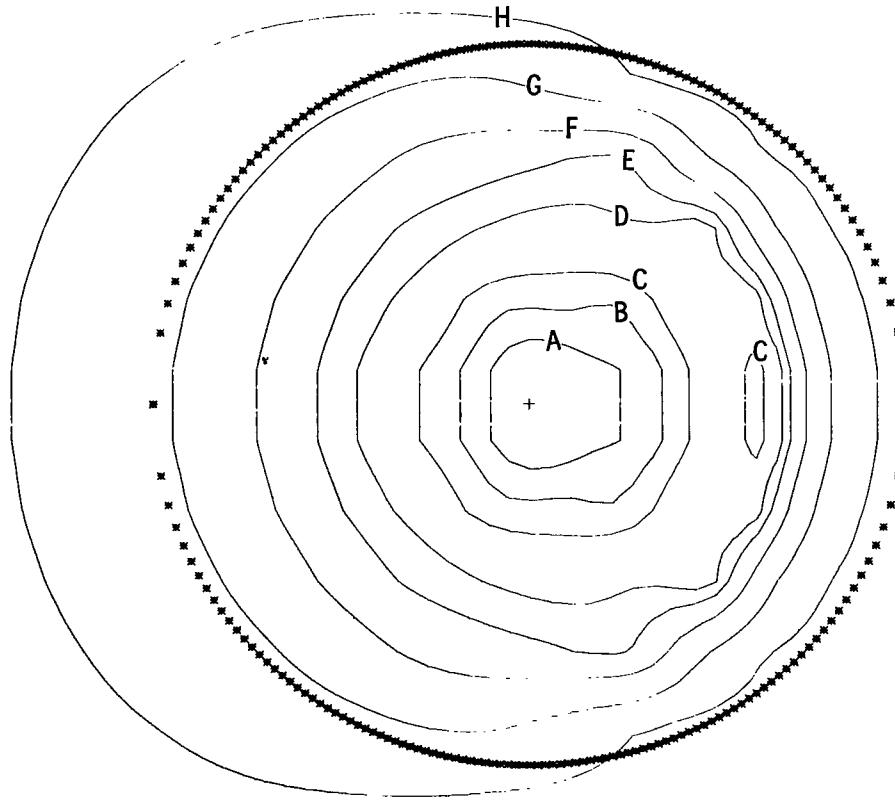

(b) m = 2.

Figure 3. - Continued.

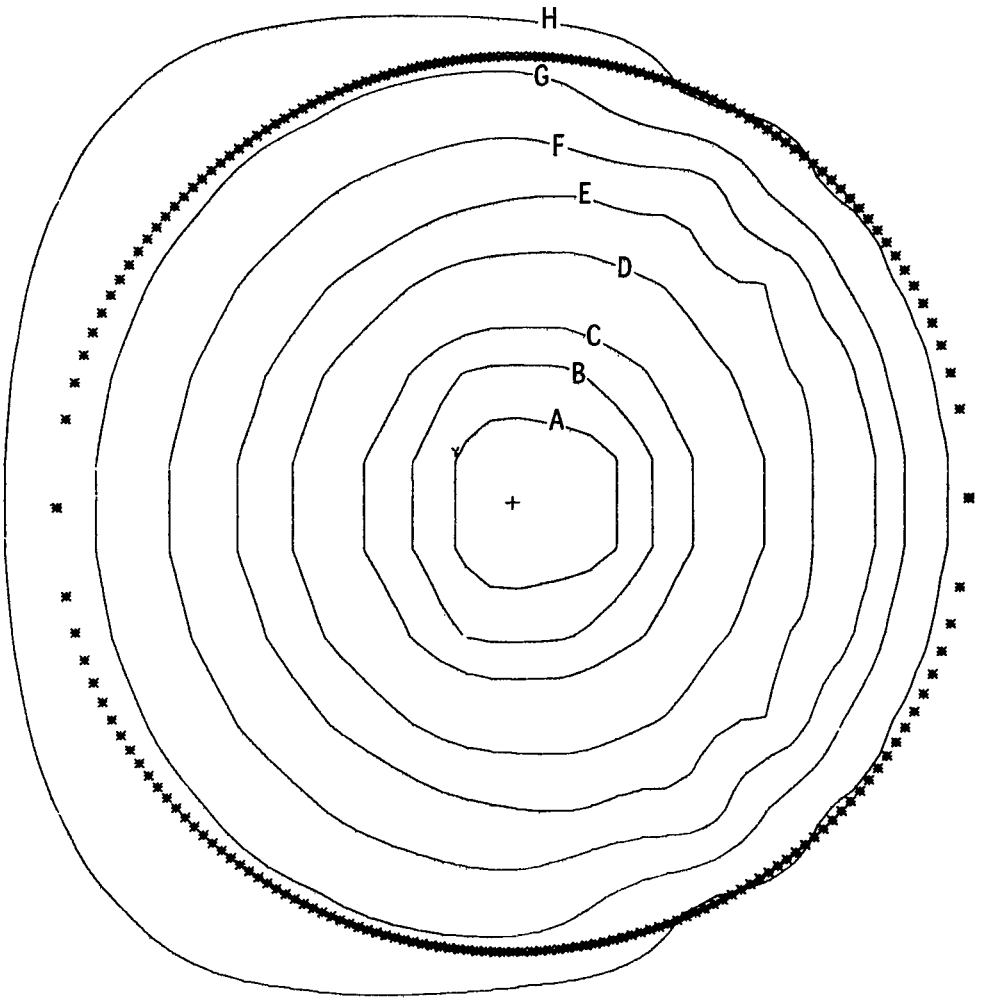

(c) m = 1.25.

Figure 3. - Concluded.

Dimensionless
film thickness,
$H = h/R_x$

A	6.5×10^{-6}
B	7.0
C	7.5
D	8.0
E	8.5
F	8.0
G	10.0
H	11.5

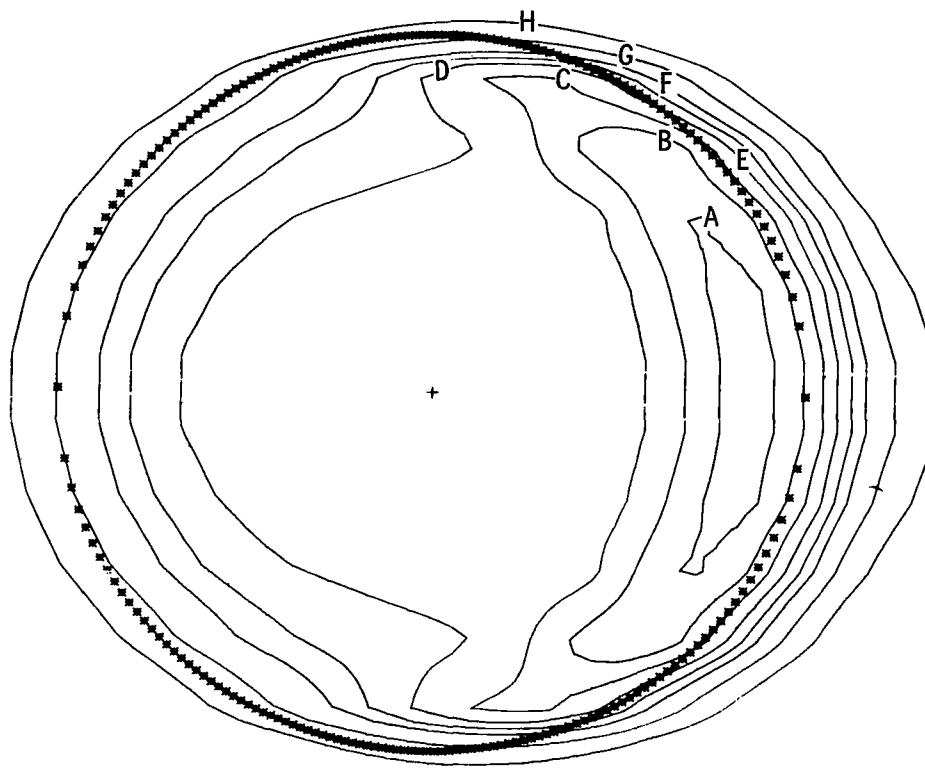

(a) m = 4.

Figure 4. - Contour plots of dimensionless film thickness for dimensionless inlet distances m of 4, 2, and 1.25 and for group 1 of table II.

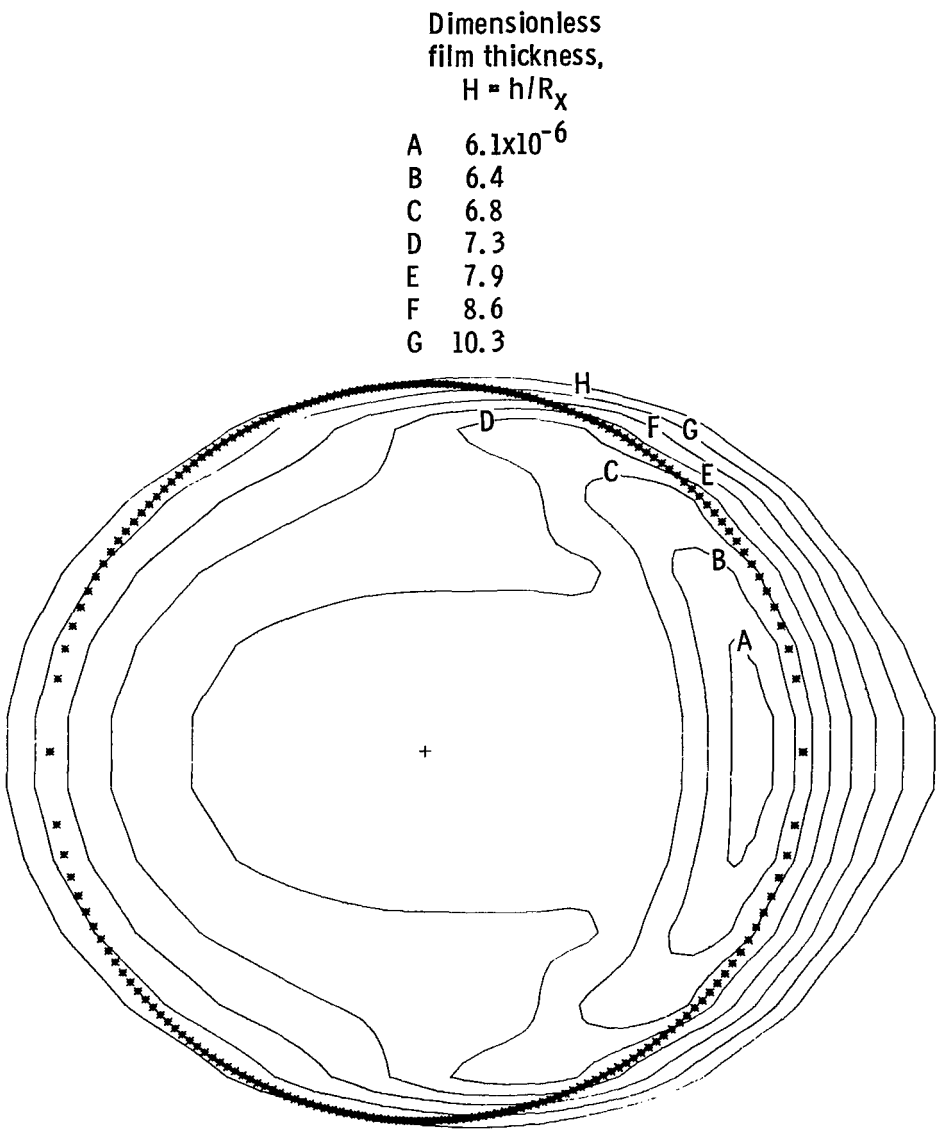

(b) m = 2.

Figure 4. - Continued.

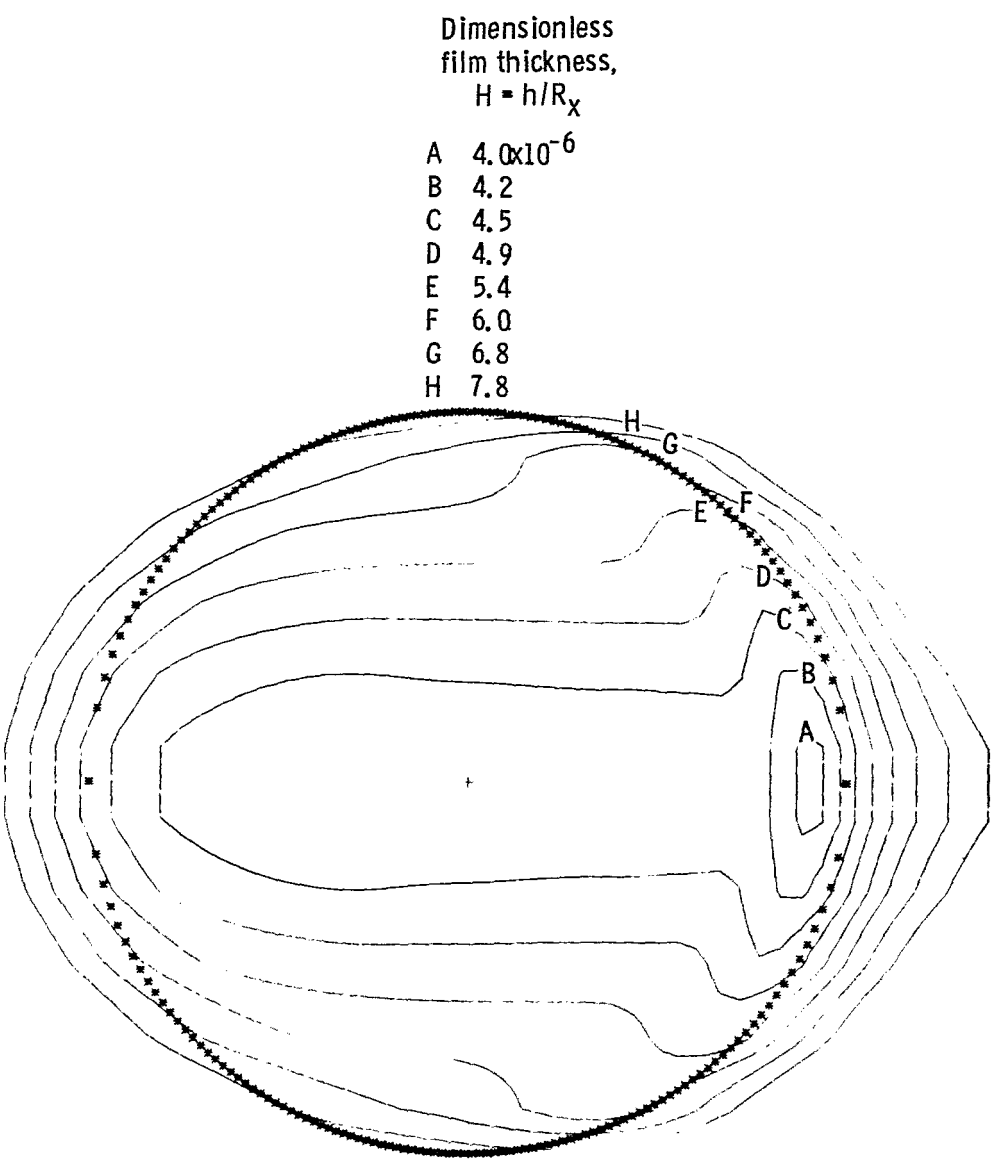

(c) m = 1.25.

Figure 4. - Concluded.

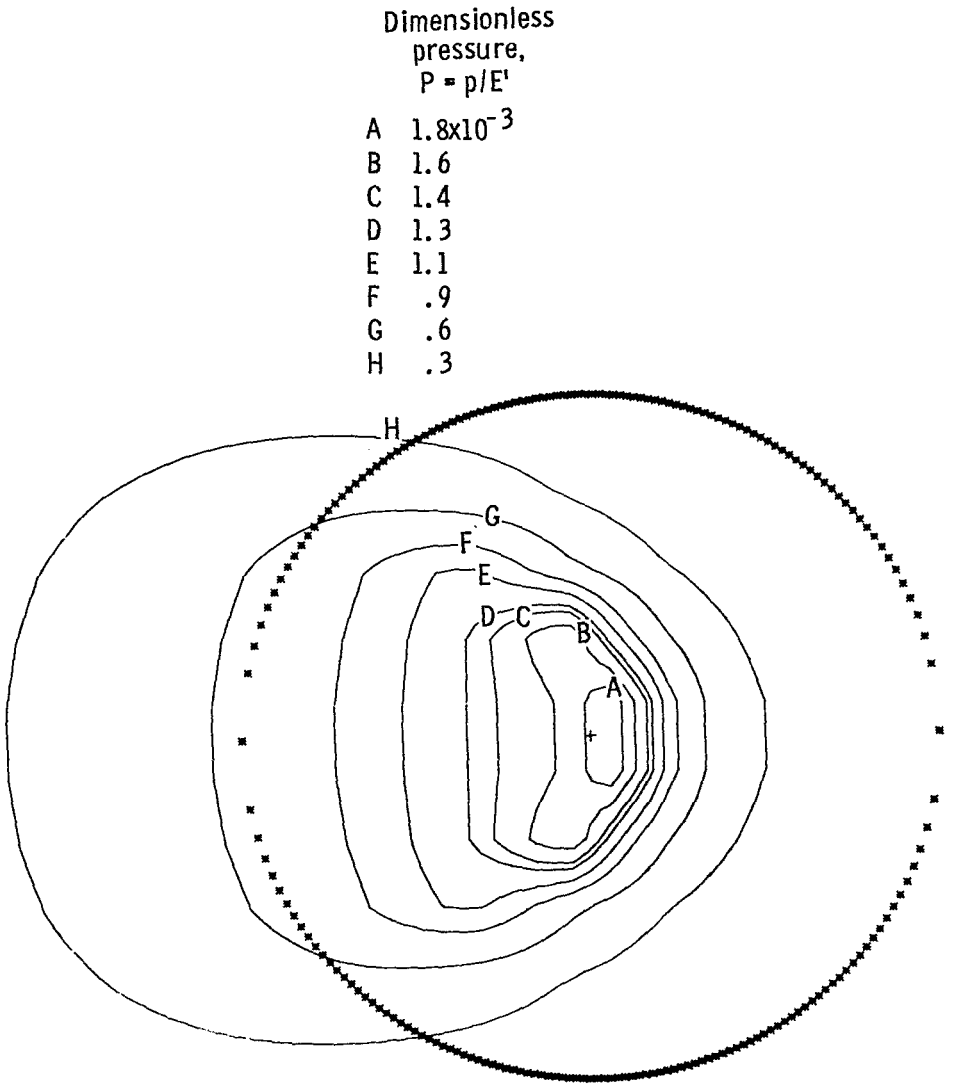

(a) m = 6.

Figure 5. - Contour plots of dimensionless pressure for dimensionless inlet distances m of 6, 2.5, and 1.5 and for group 3 of table II.

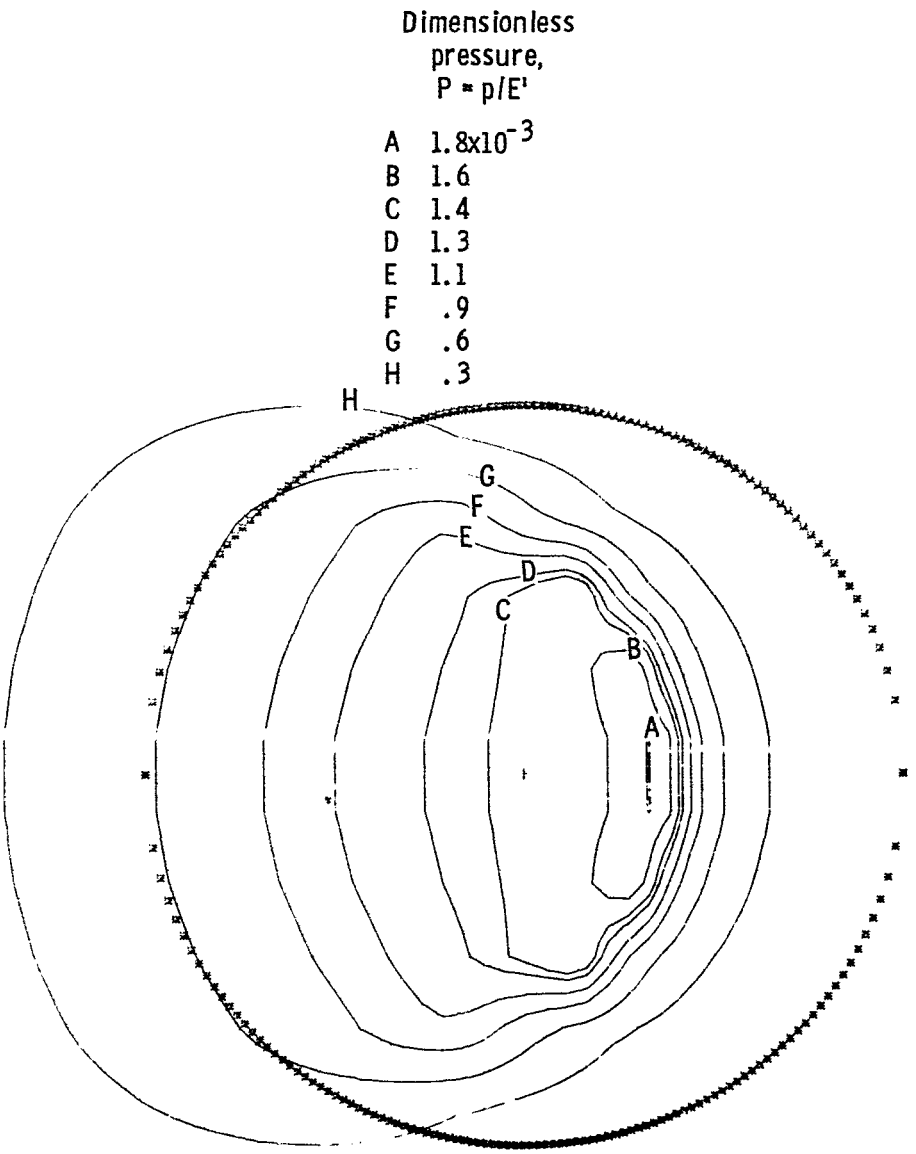

(b) m = 2.5.

Figure 5. - Continued.

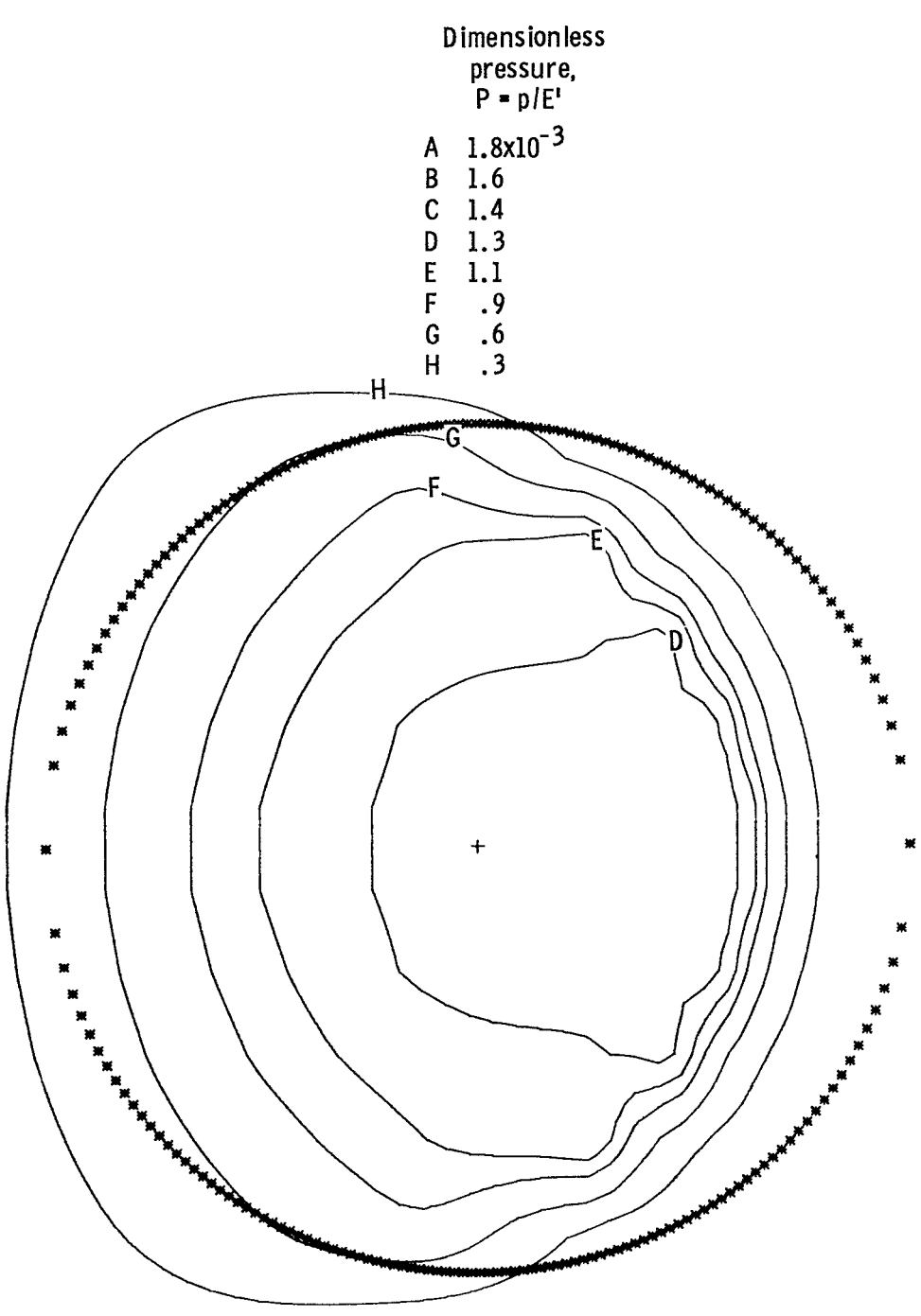

(c) m = 1.5.

Figure 5. - Concluded.

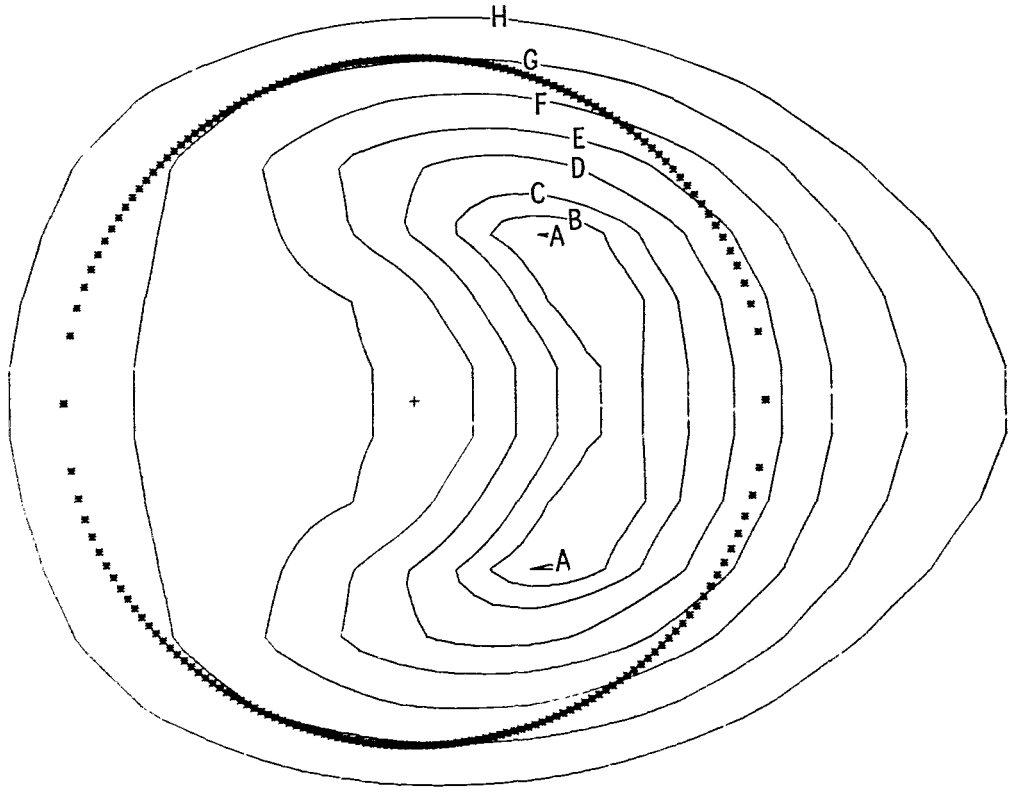

(a) m = 6.

Figure 6. - Contour plots of dimensionless film thickness for dimensionless inlet distances m of 6, 2.5, and 1.5 and for group 3 of table II.

Dimensionless
film thickness,
$H = h/R_x$

A	47.0×10^{-6}
B	47.5
C	48.0
D	49.0
E	51.0
F	54.0
G	58.0
H	63.0

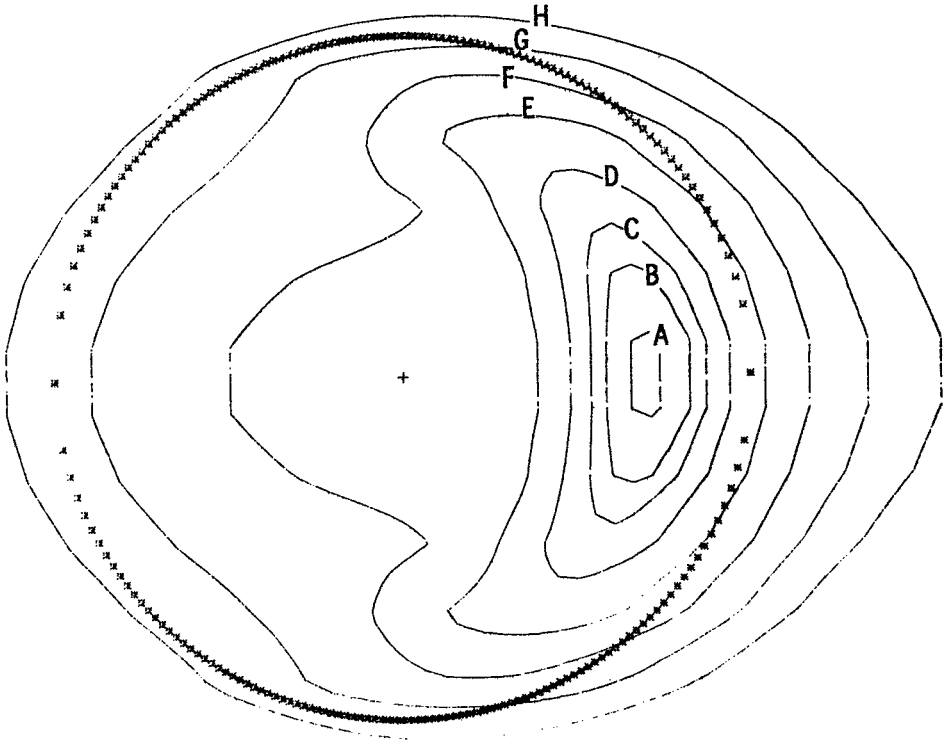

(b) m = 2.5.

Figure 6. - Continued.

Dimensionless
film thickness,
$H = h/R_x$

A	28.0×10^{-6}
B	28.5
C	29.0
D	30.0
E	32.0
F	35.0
G	39.0
H	44.0

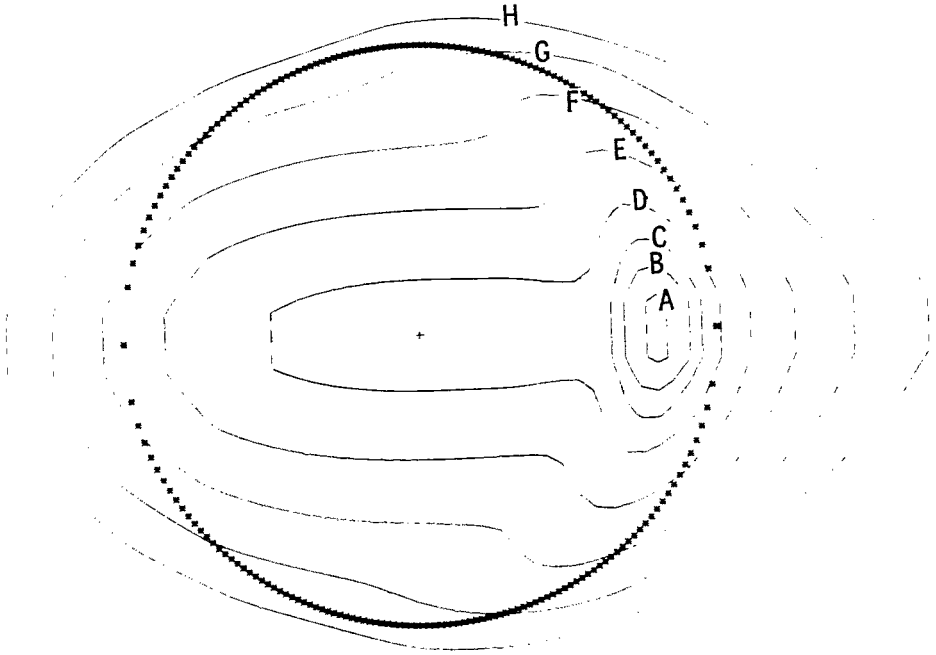

(c) m = 1.5.

Figure 6. - Concluded.

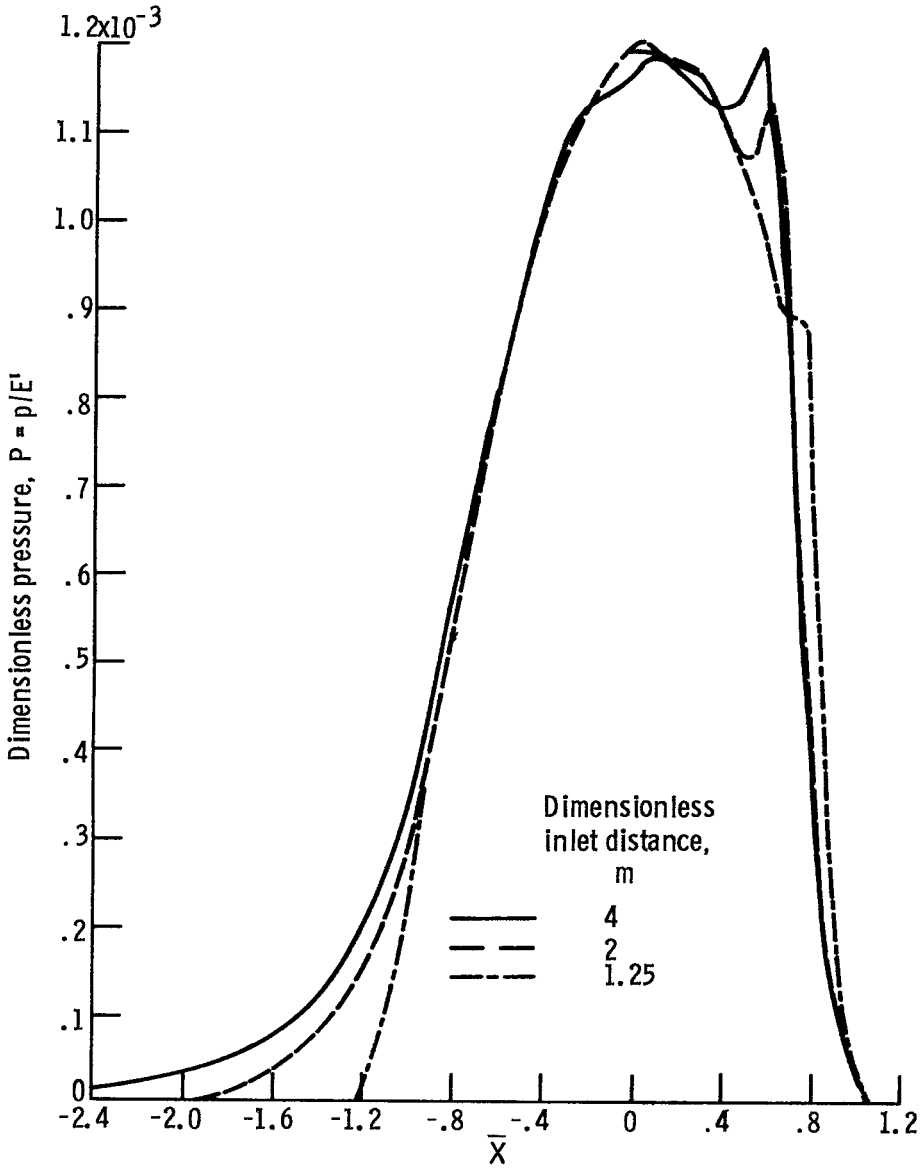

(a) Dimensionless parameters U and W held constant as given in group 1 of table II.

Figure 7. - Dimensionless pressure on $\bar{X}$-axis for three values of dimensionless inlet distance. The value of $\bar{Y}$ is held fixed near axial center of contact.

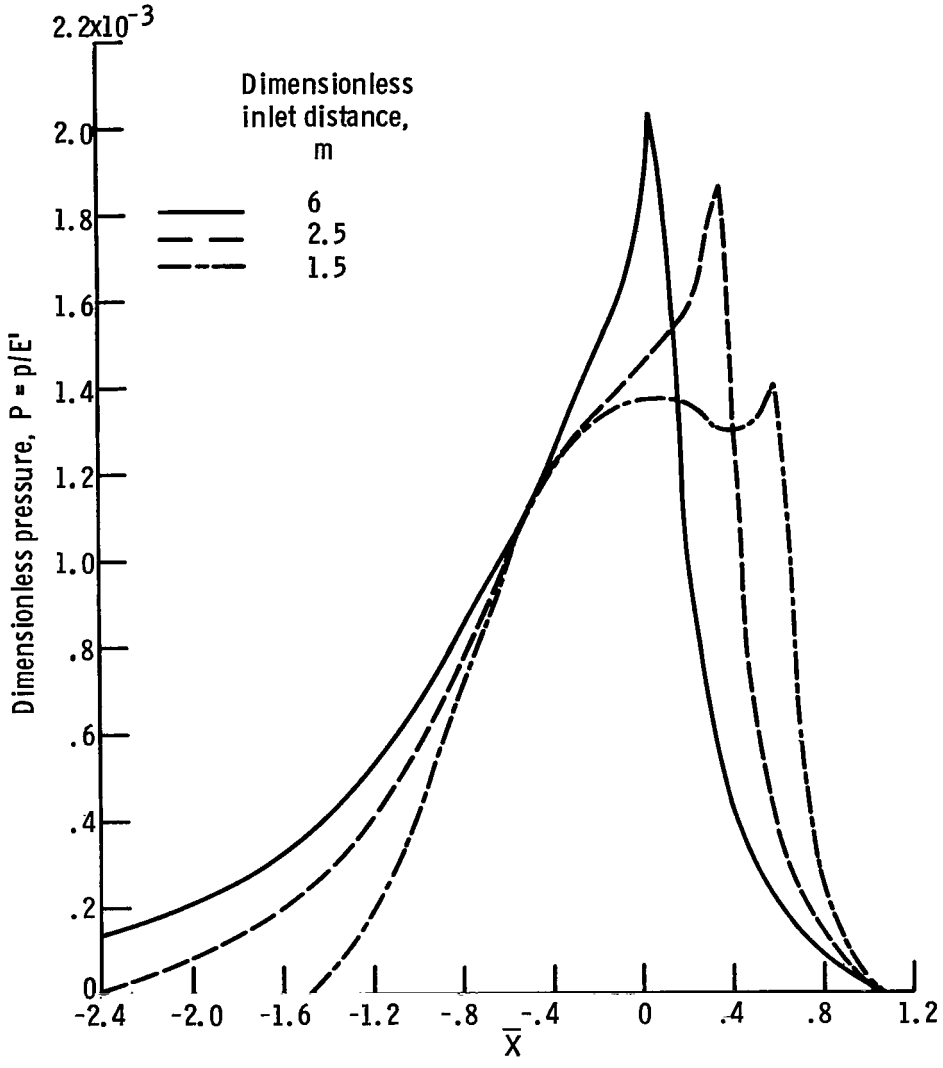

(b) Dimensionless parameters U and W held constant as given in group 3 of table II.

Figure 7. - Concluded.

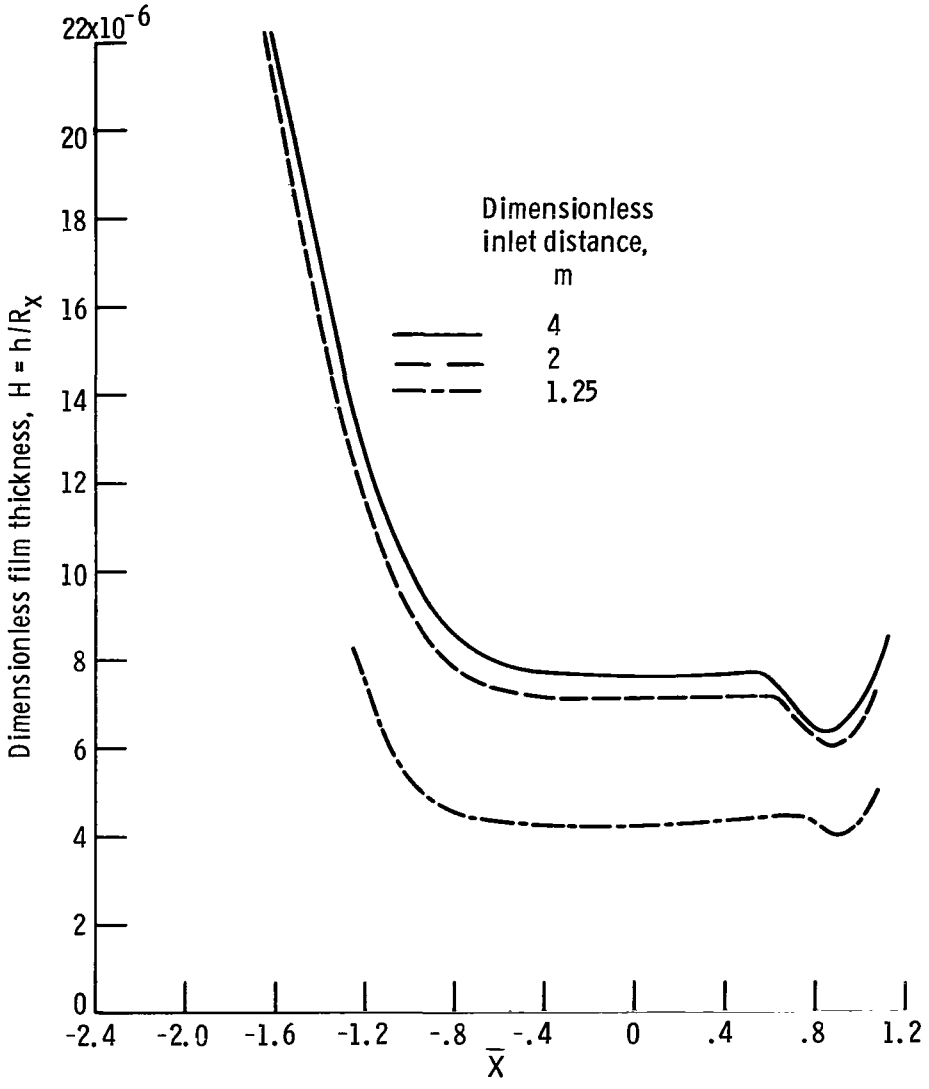

(a) Dimensionless parameters U and W held constant as given in group 1 of table II.

Figure 8. - Dimensionless film thickness on $\bar{X}$-axis for three values of dimensionless inlet distance. The value of $\bar{Y}$ is held fixed near axial center of contact.

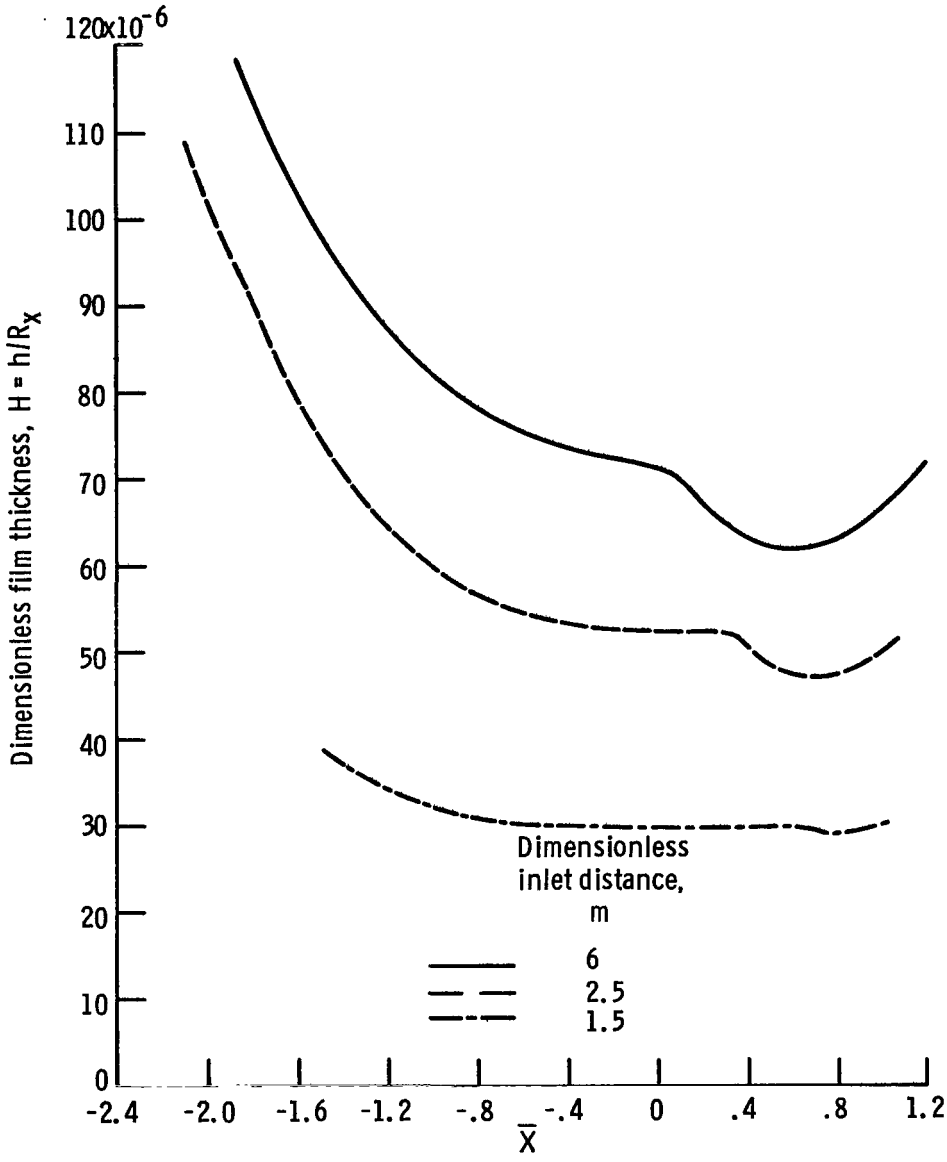

(b) Dimensionless parameters U and W held constant as given in group 3 of table II.

Figure 8. - Concluded.

"The aeronautical and space activities of the United States shall be conducted so as to contribute . . . to the expansion of human knowledge of phenomena in the atmosphere and space. The Administration shall provide for the widest practicable and appropriate dissemination of information concerning its activities and the results thereof."

—NATIONAL AERONAUTICS AND SPACE ACT OF 1958

NASA SCIENTIFIC AND TECHNICAL PUBLICATIONS

TECHNICAL REPORTS: Scientific and technical information considered important, complete, and a lasting contribution to existing knowledge.

TECHNICAL NOTES: Information less broad in scope but nevertheless of importance as a contribution to existing knowledge.

TECHNICAL MEMORANDUMS: Information receiving limited distribution because of preliminary data, security classification, or other reasons. Also includes conference proceedings with either limited or unlimited distribution.

CONTRACTOR REPORTS: Scientific and technical information generated under a NASA contract or grant and considered an important contribution to existing knowledge.

TECHNICAL TRANSLATIONS: Information published in a foreign language considered to merit NASA distribution in English.

SPECIAL PUBLICATIONS: Information derived from or of value to NASA activities. Publications include final reports of major projects, monographs, data compilations, handbooks, sourcebooks, and special bibliographies.

TECHNOLOGY UTILIZATION PUBLICATIONS: Information on technology used by NASA that may be of particular interest in commercial and other non-aerospace applications. Publications include Tech Briefs, Technology Utilization Reports and Technology Surveys.

Details on the availability of these publications may be obtained from:

SCIENTIFIC AND TECHNICAL INFORMATION OFFICE

NATIONAL AERONAUTICS AND SPACE ADMINISTRATION

Washington, D.C. 20546